Separation and Purification Technology 235 (2020) 116117

Contents lists available at ScienceDirect

Separation and Purification Technology

journal homepage: www.elsevier.com/locate/seppur

Impact of phosphate, silicate and natural organic matter on the size of Fe(III) precipitates and arsenate co-precipitation efficiency in calcium containing water

Arslan Ahmad[a,b,c,d,*], Sam Rutten[c], Martijn Eikelboom[c], Luuk de Waal[a], Harry Bruning[c], Prosun Bhattacharya[b,e], Albert van der Wal[c,d]

[a] KWR Water Cycle Research Institute, Nieuwegein, the Netherlands
[b] KTH-International Groundwater Arsenic Research Group, Department of Sustainable Development, Environmental Science and Engineering, KTH Royal Institute of Technology, Stockholm, Sweden
[c] Department of Environmental Technology, Wageningen University and Research (WUR), Wageningen, the Netherlands
[d] Evides Water Company N.V., Schaardijk 150, 3063 NH Rotterdam, the Netherlands
[e] International Centre for Applied Climate Science, University of Southern Queensland, Toowoomba, Australia

ARTICLE INFO

Keywords:
Arsenic removal
Drinking water
Groundwater treatment
Ferric chloride ($FeCl_3$)
Natural organic matter (NOM)

ABSTRACT

Removal of arsenic (As) from water by co-precipitation with Fe(III) (oxyhydr)oxides is a widely used technique in water treatment. Nevertheless, As removal efficiency appears to be sensitive to the composition of the water matrix. The aim of this study was to gain a deeper understanding of the independent and combined effects of silicate (Si), phosphate (P), natural organic matter (NOM) and calcium (Ca) on arsenate [As(V)] co-precipitation efficiency and the size of Fe(III) precipitates. We found that, in complex solutions, containing multiple solutes and high levels of Ca, (variations in) Si and P concentrations reduce As(V) removal to some extent, mainly due to a decreased adsorption of As(V) onto Fe(III) precipitates. On the other hand, NOM concentrations reduced As(V) removal to a much greater extent, due to possible formation of mobile Fe(III)–NOM complexes that were difficult to remove by filtration. These findings have a great significance for predicting As(V) removal as a function of seasonal and process-related water quality changes at water treatment plants.

1. Introduction

The co-precipitation of arsenic (As) with *in situ* produced Fe(III) (oxyhydr)oxides is a widely used As removal technique in water treatment [11,29,38]. Typically, an Fe(III) coagulant such as ferric chloride ($FeCl_3$) is dosed which, in contact with water, undergoes hydrolysis to form Fe(III)(oxyhydr)oxide precipitates. Arsenic adsorbs onto the surface of the Fe(III) precipitates, at an early stage of the precipitate growth [16,18,28,38,42]. The As bearing Fe(III) precipitates (i.e. co-precipitated As and Fe(III)) can be removed from water in a downstream granular media filter or e.g. with low-pressure membranes [4,19]. At pH relevant to most natural waters (6.5–8.5), As(V) is negatively charged and therefore exhibits a higher affinity for the surface of Fe(III) precipitates than As(III) which is uncharged [16,23,33]. Therefore, in order to effectively remove As from ground water, oxidizing As(III) to As(V) e.g. by adding potassium permanganate ($KMnO_4$) before co-precipitation with Fe(III)(oxyhydr)oxides has previously been suggested [1,12,13,34]. Recent studies have shown that As(III) also oxidizes rapidly to As(V) during rapid sand filtration (RSF), a treatment step commonly used at water treatment plants [1,14,15]. Thus, the use of $KMnO_4$ in water treatment can be avoided by treating the RSF effluent for As(V) removal instead of treating the raw groundwater for As (III) removal.

The removal efficiency of As(V) with Fe(III) based co-precipitation is sensitive to the ionic composition of water [5,9,12,13,21,22,28]. The most abundant oxyanions that may impact As(V) removal are silicate (i.e.H_4SiO_4) and phosphate (i.e. $H_2PO_4^-$ or HPO_4^{2-}), denoted further as Si and P respectively [20,27,38,40]. Moreover, natural organic matter (NOM), especially humic substances (HS), can adversely affect As(V) removal [5,32,44]. These inorganic and organic solutes can modify the structure, composition and identity of the Fe(III) precipitates, thereby affecting their size and As(V) uptake behaviour [35,40]. Moreover, these solutes compete with As(V) for adsorption sites on Fe(III) precipitates [3,7,16,27,37,44,45,46]. On the other hand,

* Corresponding author at: KWR Water Cycle Research Institute, Groningenhaven 7, 3433 PE Nieuwegein, the Netherlands
E-mail address: arslan.ahmad@kwrwater.nl (A. Ahmad).

https://doi.org/10.1016/j.seppur.2019.116117
Received 1 May 2019; Received in revised form 14 September 2019; Accepted 20 September 2019
Available online 23 September 2019
1383-5866/ © 2019 The Authors. Published by Elsevier B.V. This is an open access article under the CC BY-NC-ND license (http://creativecommons.org/licenses/BY-NC-ND/4.0/).

natural waters often contain calcium ions (Ca^{+2}, denoted further as Ca), which can increase As(V) removal during Fe(III) based co-precipitation. It has been shown that Ca increases the size of Fe(III) precipitates [2] and also results in an increased uptake of As(V) by Fe(III) precipitates. Several mechanisms have been proposed to explain these observations, such as neutralization of the Fe(III) precipitate surface charge by Ca [45], suppression of electrostatic repulsion [25] and the formation of ternary complexes between Fe(III), As(V) and Ca [21], van Genuchten et al. [39].

So far, most of the available studies have focused on the interactions between As(V) and Fe(III) precipitates in simple solutions [24,43,44], whereas systematic studies providing understanding of the As(V)–Fe (III) interactions in complex multi-solute solutions are lacking. In this study, we aim to provide more insights into the independent and combined effects of Si, P, NOM and Ca on As(V) co-precipitation efficiency and the size of formed Fe(III) precipitates.

2. Materials and methods

2.1. Chemicals and stock solutions

All chemicals were reagent grade and used without any purification. The stock solutions of 1.4 g/L $FeCl_3$, 92.9 g/L $NaHCO_3$, 15 g/L NaCl, and 30.2 g/L Na_2SiO_3 were prepared by dissolving the required amounts of $FeCl_3{\cdot}6H_2O$ (CAS: 10025-77-1, 97% purity, J.T Baker The Netherlands), $NaHCO_3$ (CAS: 144–55-8, > 99% purity, J.T Baker The Netherlands), NaCl (CAS: 7647–14-5, 99% purity, J. T Baker The Netherlands) and $Na_2SiO_3{\cdot}5H_2O$ (CAS: 10213–79-3, 99% purity, Sigma-Aldrich) respectively in ultrapure water (Mill-Q, produced by purifying distilled water with a Purelab Chorus provided by Veolia). The stock solutions of 73.8 g/L $CaCl_2$, 39.2 g/L $MgCl_2$ and 0.45 g/L NaH_2PO_4 were prepared by dissolving $CaCl_2$ anhydrous (CAS: 10043-52-4, 96% purity, J. T Baker), $MgCl_2{\cdot}6H_2O$ (CAS: 7791-18-6, 99% purity, Boom B.V.) and $NaH_2PO_4{\cdot}H_2O$ (CAS: 10049-21-5, > 98% purity, J.T Baker) respectively in 0.1 M HCl. The NOM stock solution of 2.4 g DOC/L was prepared by diluting a primary stock (HumVi, Vitens, The Netherlands, 117.4 g DOC/L) that contained ca. 75% HS (LC-OCD results given in Table S1). Arsenate was dosed using a stock solution of 1.0 g/l As_2O_5 (CAS: 12044–50-7, 99% purity, Inorganic Ventures). pH was adjusted with 0.1 M HCl or 0.1 M NaOH.

2.2. Composition of initial solutions

The experiments were performed with synthetic solutions and real RSF effluent collected from WTP Ouddorp (Table 1). The ionic composition of the synthetic initial solutions in the experiments (Table 1) was based on the yearly variation recorded in the quality of RSF effluent at the WTP (Table S2). The synthetic initial solution in the reference experiment contained 0.07 μM As(V) and 2000 μM Ca, without Si, P and NOM. The rest of the experiments are identified by the ions added in μM to the reference solution (i.e. 70Si consists of 70 μM Si, 0.07 μM As(III) and 2000 μM Ca). All the synthetic initial solutions also contained 4.1 mM $NaHCO_3$ and 0.6 mM NaCl to provide alkalinity and ionic strength.

The experiments with the RSF effluent were performed with and without pre-treatment with anion exchange (AEX) or cation exchange (CEX). The objective of the AEX or CEX pre-treatment was to remove the naturally present anions or cations from the RSF effluent before use as initial solution in the experiments, to determine the impact of natural anions or cations on Fe(III) precipitation and As(V) removal. The AEX was performed with Amberlite® IRA-400 chloride form resin (CAS: 60177–39-1) and the CEX was carried out with Amberlite® IR120 N^+ form (CAS: 68441-33-8), both were obtained from Sigma Aldrich, Zwijndrecht, The Netherlands. Each IEX treatment was performed in a glass column with a contact time of 1 min and bed volumes of 78 cm^3. The RSF effluent based initial solutions were spiked with As(V) to achieve As concentration of 0.07 μmol/L (i.e. similar As concentration as synthetic initial solutions). The AEX effluent samples were dosed with $NaHCO_3$ to compensate for the loss of HCO_3 during AEX.

Table 1
Nomenclature and composition of the initial solutions used in the co-precipitation experiments. In all the initial solutions the concentration of Fe(III) was 5 μmol/L, As(V) was 0.07 μmol/L (As/Fe = 0.014) and HCO_3 was 4100 μmol/L. The concentration of Ca was 2000 μmol/L in all the synthetic initial solutions (Ca/Fe = 400). In RSF effluent the concentration of Ca was 2200 μmol/L (Ca/Fe = 440), which was reduced to < 1 μmol/L after CIEX treatment.

Experiment code	Si	P	DOC	Si/Fe	P/Fe	DOC/Fe
	μmol/L			mol/mol		
Reference (Ref)	–	–	–	–	–	–
Si70	70	–	–	14	–	–
Si140	140	–	–	28	–	–
Si280	280	–	–	56	–	–
P1.3	–	1.3	–	–	0.26	–
P2.5	–	2.5	–	–	0.5	–
P3.3	–	3.3	–	–	0.66	–
DOC165	–	–	165	–	–	33
DOC330	–	–	330	–	–	66
DOC500	–	–	500	–	–	100
Si0 + P1.3 + DOC165	–	1.3	165	–	0.26	33
Si140 + P1.3 + DOC165	140	1.3	165	28	0.26	33
Si280 + P1.3 + DOC165	280	1.3	165	56	0.26	33
Si140 + P2.5 + DOC165	140	2.5	165	28	0.5	33
Si140 + P3.3 + DOC165	140	3.3	165	28	0.66	33
Si140 + P1.3 + DOC330	140	1.3	330	28	0.26	66
Si140 + P1.3 + DOC500	140	1.3	500	28	0.26	100
Effluent RSF[+]	153	1.5	172	31	0.3	34
Effluent RSF after CIEX[+]	159	1.5	175	32	0.3	35
Effluent RSF after AIEX[+] *	160	BDL	59	32	–	12

BDL: below detection limit (< 0.2 μmol/L).
* HCO_3 was compensated after the AIEX treatment.
[+] As(V) was spiked using a stock solution.

2.3. Co-precipitation experiments

The experiments were performed with a 5 L glass reactor connected to a controller (ez-Control, Applikon® Biotechnology) for adjusting, maintaining and logging (BioXpertV2 software) reaction parameters, including the pH, temperature, oxidant supply and stirring speed (Fig. 1). The reactor was connected to a Mastersizer 2000 (Malvern Instruments, UK). The experiments were carried out at pH 7.5 and 20 °C, with stirring set to 100 rpm. The experimental procedure included: (i) preparation of the initial solutions in the reaction vessel and collection of solution samples for control, (ii) dosing the $FeCl_3$ stock to result in Fe(III) concentration of 5 μmol/L and allowing the hydrolysis and precipitation of Fe(III) to take place while the suspension was stirred at 100 rpm and (iii) collection of suspension samples after 1 and 60 min of $FeCl_3$ addition, which were filtered over 0.45 μm filters to determine the removal of Fe(III) precipitates. The samples were preserved for subsequent analysis. The unfiltered samples without conservation were collected for zeta-potential measurements.

For the filtration of samples Spartan™ 30/0.45 RC 0.45 μm syringe filters (GE Healthcare, Buckinghamshire, UK) were used. Samples for Fe, As, Si, Ca and P were conserved by addition of 50 μL 60% HNO_3 solution to 50 mL of sample and stored at 4 °C. The removal of As and Fe were determined from the difference between the measured values of the initial solution and final filtered solution. Samples for DOC analysis were conserved by adding 200 μL 40% HCl solution to 100 mL of sample which was closed off airtight and stored at 4 °C.

2.4. Wet analysis

Arsenic, Fe, Ca, Si, P were measured in water samples by Inductively

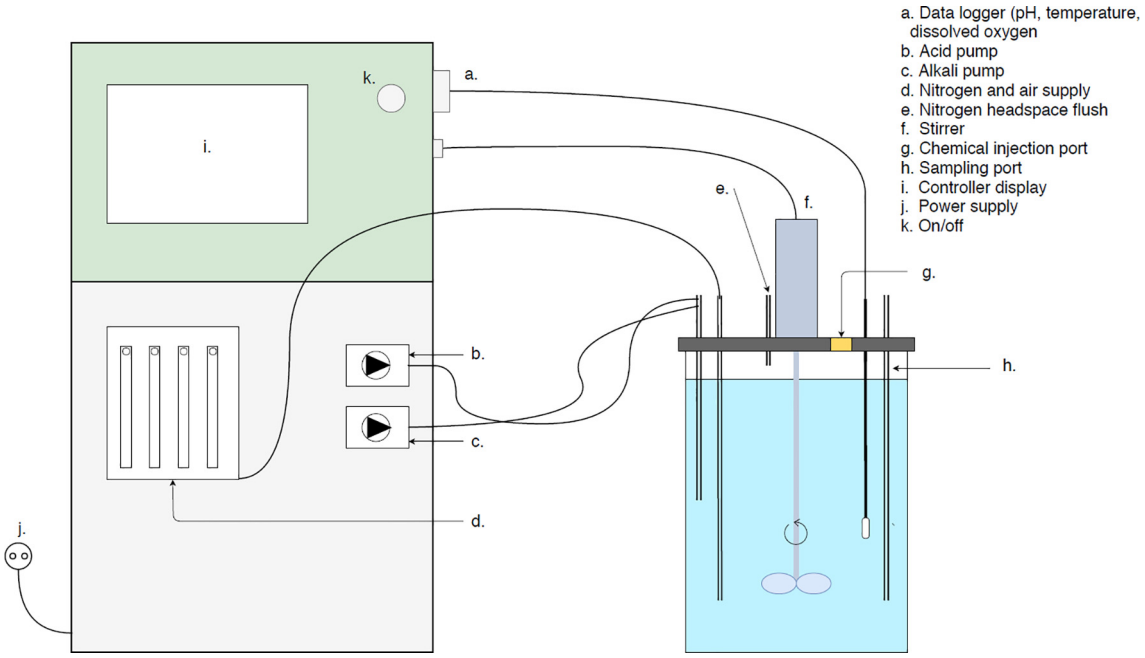

Fig. 1. A schematic overview of the laboratory setup.

Coupled Plasma Mass Spectrometry (ICP-MS) (XSERIES 2, Thermo Fisher Scientific, The Netherlands). The analysis of DOC in water samples was carried out with a Shimadzu TOC-V_{CPH} total organic carbon analyzer (Shimadzu Benelux, 's-Hertogenbosch, The Netherlands). Bicarbonate was analyzed by colorimetric method (HI-3811, Hanna Instruments).

2.5. Particle characterization

The size distribution of the Fe(III) precipitates was determined by Multiple Light Scattering (MLS) using the Mastersizer 2000 (Malvern Instruments, UK). The Mastersizer was connected to the co-precipitation reactor and the suspension was fed to the Mastersizer at a constant flow of 216 mL/min through a masterflex easy-load II peristaltic pump combination (Metrohm Nederland B.V. The Netherlands). Malvern instruments mastersizer 2000 software v5.61 recorded the particle size distribution every 20 s for 5 min. The Zetasizer Nano-ZS (Malvern Instruments) was used for the determination of electrophoretic mobility and the calculated zeta-potential of the particles in a sub-set of samples collected after 60 min of $FeCl_3$ dosing. Each sample was equilibrated at 20 °C for 300 s prior to measurement which were obtained in duplicate. The measurement cell (cuvette) was rinsed with ethanol and demineralized water and dried between the measurements.

3. Results and discussion

3.1. Size distribution and filterability of Fe(III) precipitates

3.1.1. Impact of independent Si, P and NOM addition

The particle size distribution and the removal efficiency of Fe(III) precipitates by 0.45 μm filters as a function of the composition of initial solution are given in Figs. 2 and 3 respectively. For the reference experiment, (initial solution free of Si, P and NOM), the particles were in the range of 5–180 μm with the mode of the distribution (d_m, the most commonly occurring particle diameter) at 70 μm. The precipitates in both 1 min and 60 min samples were completely removed (≈100% removal) by 0.45 μm filtration, indicating a rapid growth of Fe(III) precipitates within the first minute. When different concentrations of Si or P were added, the size distribution of the precipitates was not significantly affected, although a slightly lower d_m (≈ 50 μm) was noted for the highest Si and P additions (i.e. 280 Si μM and 3.3 μM P) compared to the reference (d_m ≈ 70 μm). Nevertheless, the precipitates were completely removed by 0.45 μm filtration in all the samples, indicating yet effective and rapid Fe(III) precipitate growth. Silicate and P oxyanions bind to the surface of Fe(III) precipitates and result in colloidally stable suspensions [8,30]. On the other hand, it has been shown that in the presence of Ca the electrostatic repulsion between the particles is reduced, which can result in coagulation/destabilization of colloidal Fe(III) precipitates. For example, Mayer and Jarrell [26] reported an improved flocculation, settling and filtration of Fe(III) precipitates in a solution where the molar Si/Fe and Ca/Fe ratio was 4.5 and 20 (Ca/Si = 0.2). In our study, however, the molar Ca/Si ratio was much higher (Ca/Si = 7–28) than in the study of Mayer and Jarrell [26]. Similarly, Van Genuchten et al. [40], in their co-precipitation experiments, noticed a stabilization of Fe(III) suspensions at molar P/Fe ratio of 0.3 and destabilization of the colloids was observed when Ca was present at Ca/Fe = 2.0 (Ca/P = 6.7). In our study the molar Ca/P was 570–1300, thus much higher than Van Genuchten et al. [40]. From this we conclude that in our study the large size and highly efficient removal of the Fe(III) precipitates by 0.45 μm filtration with the independent additions of Si and P was due to the presence of high Ca concentration in water (Table 1).

Unlike the Si and P additions, the independent NOM addition altered the particle size distribution significantly (Fig. 2). The particle size distribution was bimodal for 330 and 500 μM DOC additions, consisting of a larger contribution from particles in the non-colloidal size range (i.e. ≥1 μm) and a relatively small contribution in the colloidal range (< 1 μm) for each case (please note that the precipitate size distribution was not measured for 165 μM DOC addition). Moreover, Fe (III) removal by 0.45 μm filtration was significantly reduced (e.g. with the additions of 165, 330 and 500 μM DOC, Fe(III) removal after 60 min was ≈ 40, 30 and 20% respectively, Fig. 3). These observations are in agreement with several previous studies which also report a similar reduction in the removal of Fe(III) in the presence NOM. The suppression of Fe(III) removal by filtration has been attributed to formation of soluble Fe(III)–NOM complexes, as well as formation of Fe(III)–NOM and Fe(III)(oxyhydr)oxide–NOM colloids [5,22,32]. These different Fe (III)–NOM complexes, which can be soluble and/or colloidal, are not removed from water by 0.45 μm filtration due to their small size. Although the exact mechanism for the decreased Fe(III) removal in the

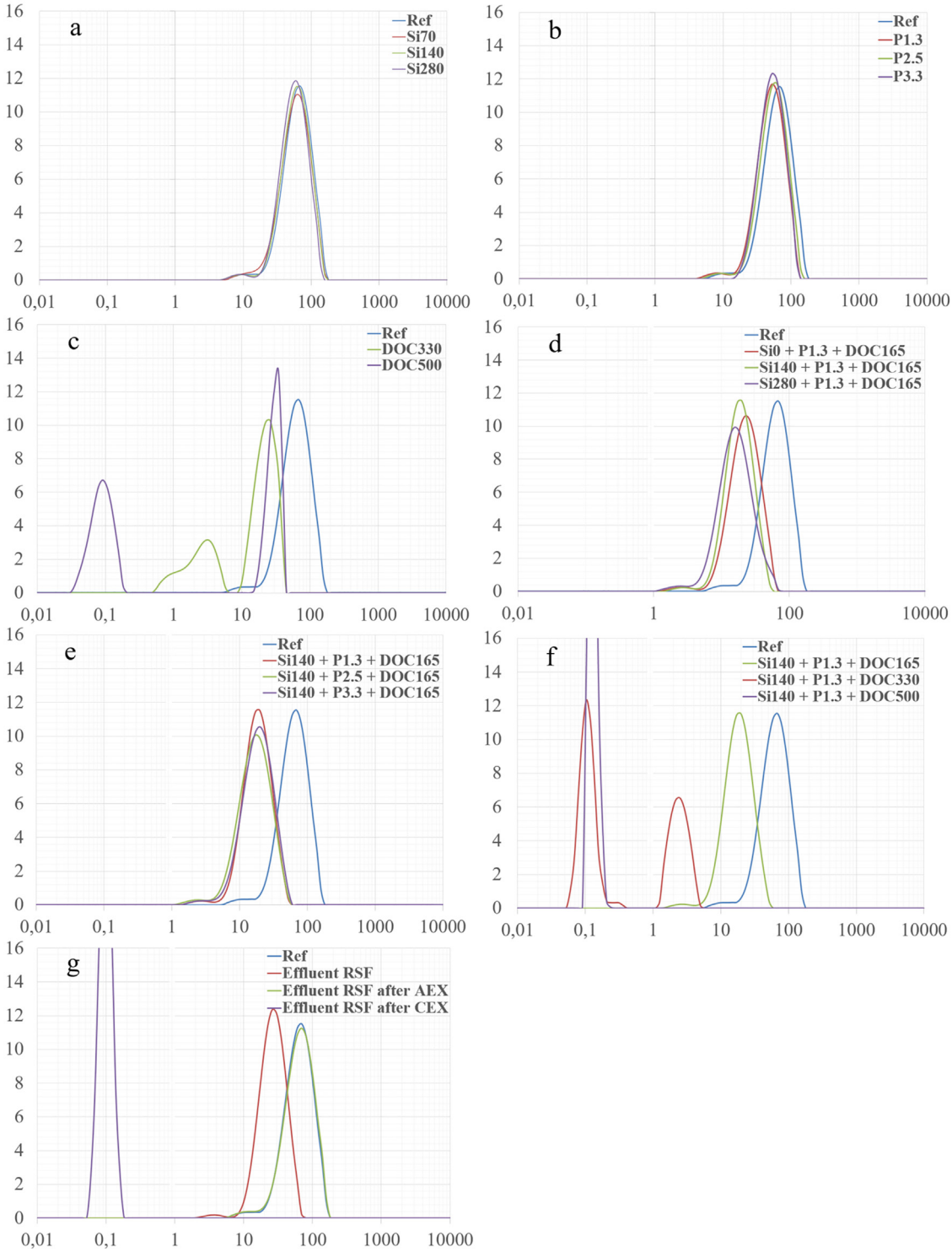

Fig 2. Independent and combined effects of silicate, phosphate and natural organic matter on Fe(III) precipitate size. X-axis: particle size (μm). Y-axis: abundance (%). *Ref* refers to the reference experiment performed in the absence of Si, P and NOM. In (Fig. 2f & g) complete Y-axis is not shown. In Fig. 2f the abundance peak of *Si140 + P1.3 + DOC 500* is at 35.4%. In Fig. 2g the abundance peak of *Effluent RSF after CEX* is at 25.5%.

presence of NOM in our study is not clarified, it is proposed that the mobility of Fe(III) was attributed to the formation of soluble and colloidal Fe(III)–NOM complexes.

To study further the precipitate aggregation, we characterized the particles from a subset of experiments by zeta-potential measurements. The zeta-potential of the reference sample was low (−2.6 mV, Table 2) and no considerable decrease was observed with the addition of 3.3 μM P (−2.8 mV). This is in agreement with the yet effective aggregation of Fe(III) precipitates with the independent P addition, similar to the reference. In the presence of 165 μM DOC the zeta-potential decreased somewhat (−11.1 mV), which is in agreement with the restricted growth of the precipitates in the presence of 165 μM DOC, due to electrostatic repulsion between the Fe(III) particles.

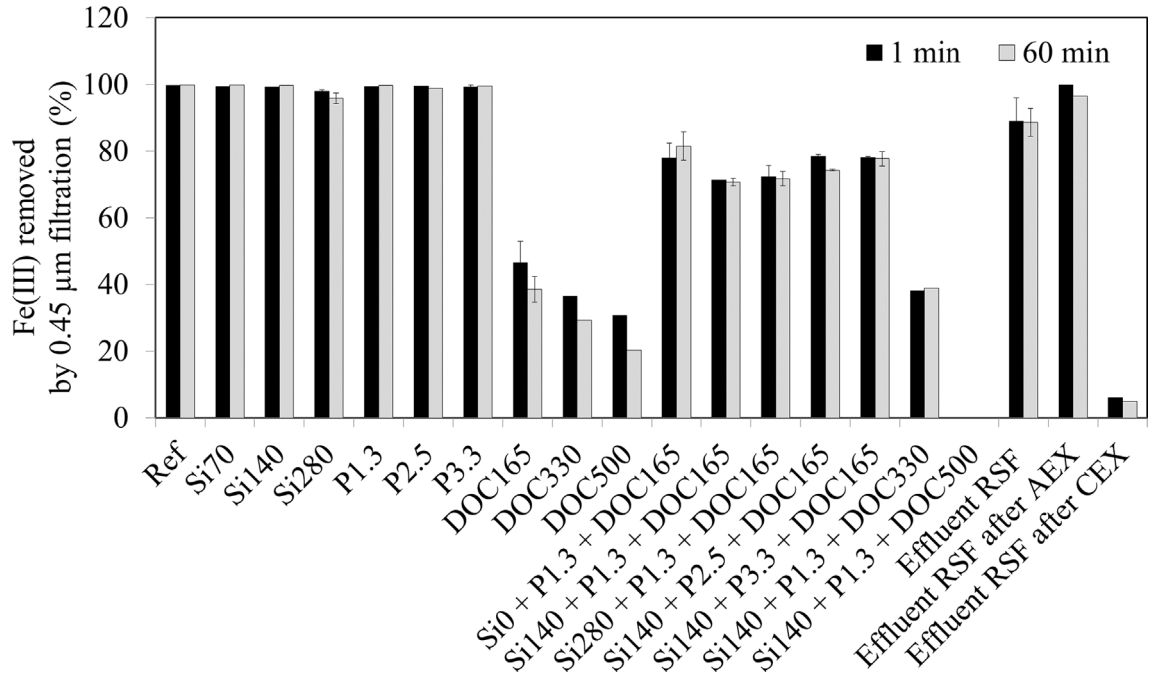

Fig. 3. Percentage Fe(III) removed by 0.45 µm filtration as a function of the composition of the initial solution and time. *Ref* refers to the reference experiment performed in the absence of Si, P and NOM.

Table 2
The zeta-potential of Fe(III) precipitates in a sub-set of experiments.

Experiment code	Zeta-potential [mV]
Reference	−2.6 ± 0.9
P3.3	−2.8 ± 0.6
DOC165	−11.1 ± 1.5
P1.3 + DOC165	−5.5 ± 1.9
Si140 + P1.3 + DOC165	−5.7 ± 0.9
Si280 + P1.3 + DOC165	−7.6 ± 0.2
Si140 + P2.5 + DOC165	−7.1 ± 0.6
Si140 + P1.3 + DOC330	−13.1 ± 0.3
RSF effluent	−7.0 ± 1.2

3.1.2. Impact of combined Si, P and NOM addition

In experiments where P and NOM were present with and without Si, the Fe(III) particles were smaller than in the reference (Fig. 2). Moreover, the removal of Fe(III) precipitates by 0.45 µm filtration was lower than the reference (≤80% compared to 100%) (Fig. 3). Minor changes in the precipitate size were observed with the variation in solution composition. For example, in the absence of Si when 1.3 µM P was present with 165 µM DOC, particles in the range of 1.4–70 µm were observed with d_m of ≈ 20 µm. The addition of 140 to 280 µM Si in this solution resulted in a very slight decrease in the removal of Fe(III) precipitates by 0.45 µm filtration (≈ 10%). Moreover, the precipitate size range was similar to the solution that did not contain Si (i.e. 1.3 µM P and165 µM DOC). Similarly, the precipitate size distribution and the removal efficiency of Fe(III) was not significantly affected in the experiments where the concentration of P was increased from 1.3 to 3.3 µM, keeping Si and DOC fixed at 140 and 165 µM respectively. Thus, the studied variations in Si and P concentrations with fixed concentrations of NOM and Ca in water, did not severely impact the size of Fe(III) precipitates.

Compared to when only NOM (165 µM DOC) was present, the Fe(III) removal by 0.45 µm filtration was higher when NOM was present with P and Si (Fig. 3). Also, the zeta-potential with the independent NOM addition was −11.1 mV, which was lower relative to the experiments in which NOM was present with Si and P (Table 2). The higher zeta-potential obviously is in agreement with the large size and higher removal of Fe(III) precipitates in the complex NOM bearing solutions (Figs. 2 and 3). However, the exact mechanism responsible for the higher zeta-potential when NOM co-occurred with Si and P is not clarified. Nevertheless, we note that the interactions between NOM and Fe(III) in the absence and presence of P and Si appear to follow different mechanisms.

When the concentration of NOM was increased (from 165 to 330 µM DOC), keeping Si and P (140 and 1.3 µM respectively) fixed, the Fe(III) removal by 0.45 µm filtration was reduced significantly. A further increase in NOM concentration (to 500 µM DOC) resulted in no Fe(III) removal (Fig. 3). This increasing mobility of Fe(III) may be attributed to the formation of soluble and colloidal Fe(III)–NOM complexes that were not removed with the 0.45 µm membrane filters. The presence of colloidal particles is also confirmed with the particle size distribution measurements (Fig. 2). However, the identity of the particles (Fe(III)–NOM or Fe(III)(oxyhydr)oxide–NOM colloids) was not investigated. Moreover, the properties of the soluble fraction of Fe(III)–NOM complexes remain unclear. Nevertheless, our results indicate that the variations in NOM concentrations, in solution with fixed concentrations of Si, P and Ca exhibit a strong impact on the size of Fe(III) precipitates and their removal.

3.1.3. Impact of removing anions and cations from RSF effluent

In the RSF effluent, the Fe(III) precipitate size ranged from 2 to 80 µm with the d_m at 25 µm (Fig. 2). The Fe(III) precipitates were effectively removed (≈ 95% removal) by 0.45 µm filtration in both 1 min and 60 min samples (Fig. 3). The removal of Fe(III) precipitates in the RSF effluent was slightly higher than the synthetic solutions that contained Si, P and NOM in comparable concentrations. This can be explained by a higher charge neutralization due to the higher Ca concentration and an additional presence of ≈ 10 mg/L magnesium (Mg) in the RSF effluent compared to the synthetic solutions (Table S2). When the RSF effluent was pre-treated with AEX, P and a major portion of the NOM (negatively charged) was removed from water (Table 1). The AEX did not remove Si (H_4SiO_4) because it is not disassociated at the given pH of 7.5 [6]. Interestingly, the precipitate size distribution was quite similar to the reference (i.e. in the absence of Si, P, NOM) and in solutions where we added Si. The removal efficiency of Fe(III) in the

AEX treated RSF effluent was clearly higher than the untreated RSF effluent (Fig. 3) which can be attributed to a lower charge repulsion between the particles in the absence of surface sorbed (negatively charged) P and NOM ions.

When the CEX treated RSF effluent, which lacked Ca and Mg ions (Table 1), was used as the initial solution in the co-precipitation experiments, the particle size decreased and the removal of Fe(III) precipitates by 0.45 µm filtration strongly depleted (Fe(III) removal < 10%). It has been shown previously that the presence of cations in solutions result in neutralization of Fe(III) precipitate surface charge and a lower electrostatic repulsion which promotes growth of Fe(III) precipitates [2,39,40]. In this study, when Ca and Mg were removed from water by CEX, the sorption of Si, P and NOM on Fe(III) precipitate surface resulted in a negatively charged precipitate surface with high electrostatic repulsion which hindered the precipitate growth [6].

3.2. Arsenic removal

3.2.1. Impact of independent Si, P and NOM additions

Arsenate removal was the highest in the reference experiment (i.e. in the absence of Si, P and NOM), with As(V) removal efficiency of 65% and ≈ 90% after 1 min and 60 min respectively (Fig. 4A). This represents a ≈ 75% of the total As(V) removed in the first minute, indicating a rapid adsorption of As(V) to Fe(III) precipitate surfaces. Since Fe(III) precipitates were completely removed by 0.45 µm filtration after both 1 min and 60 min (Fig. 3), the ≈ 25% increase in As(V) removal in reference experiment was attributed to the diffusion-controlled mass transfer of As to adsorption sites located in the internal porosity of Fe (III) precipitates (Fig. 4). The similar time-dependent As(V) adsorption kinetics observed in the presence of Si, P and NOM can also be explained by the slow transfer of As towards the internal adsorption sites (Fig. 4B). The independent additions of Si, P and NOM resulted in a lower As(V) removal efficiency compared to the reference (Fig. 4A). The addition of 70 µM Si resulted in As(V) removal efficiency of 45% and 75% after 1 min and 60 min, which decreased to ≈ 40% and 60% respectively, with the independent addition of the highest concentration of (280 µM Si). The addition of 1.3 µM P resulted in an As(V) removal efficiency of 25% and 44% after 1 min and 60 min, which decreased to ≈ 20% and 30% respectively, with the independent addition of the highest concentration of P (3.3 µM P). As the removal of Fe(III)

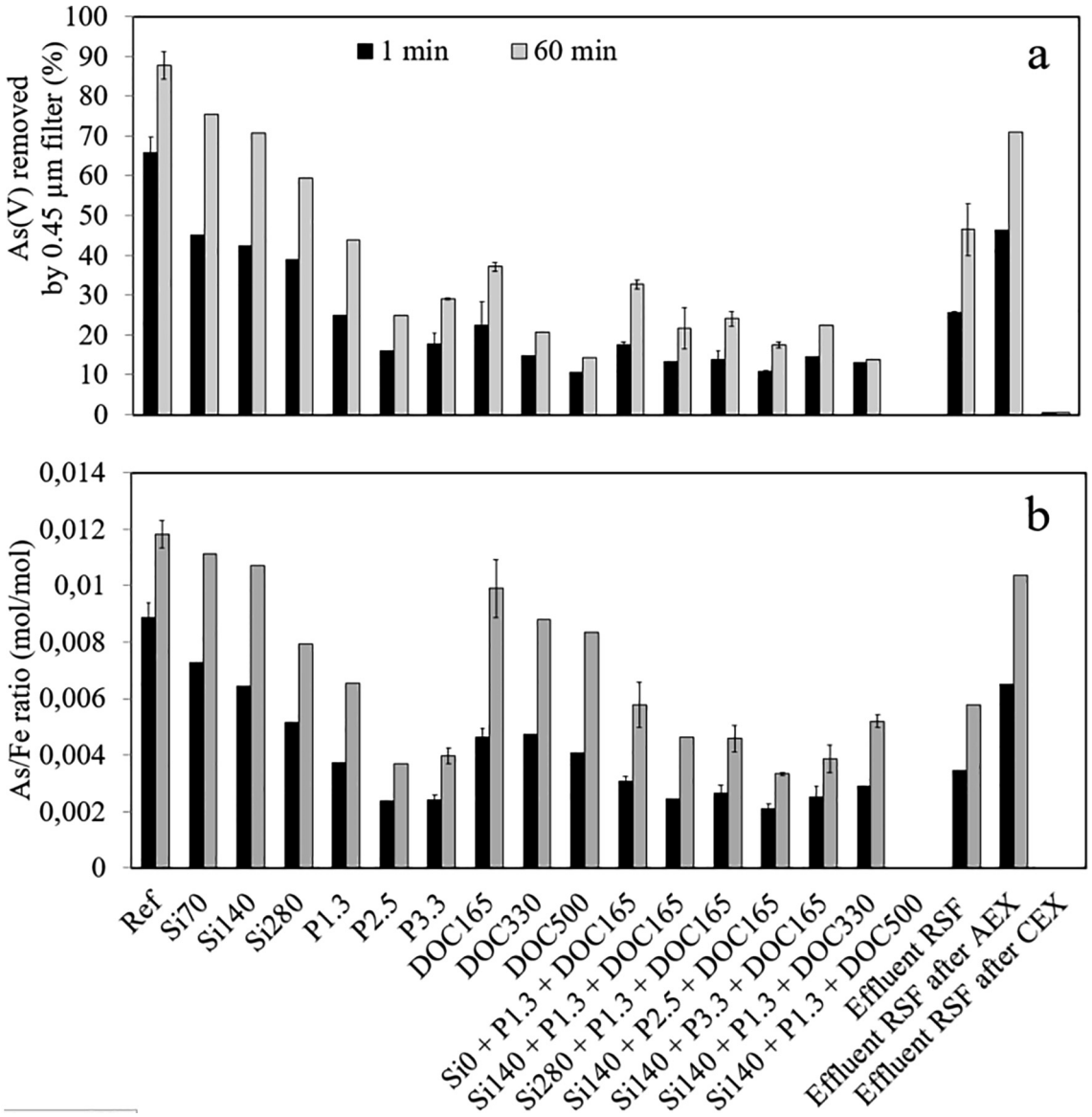

Fig 4. (a) Percentage As(V) removed by 0.45 µm filtration and (b) As(V) uptake by Fe(III) precipitates as a function of the composition of the initial solution and time. *Ref* refers to the reference experiment performed in the absence of Si, P and NOM.

precipitates by 0.45 μm filtration was (nearly) complete (Fig. 3), we conclude that the reduced As(V) removal was due to a reduced adsorption of As(V) onto the surface of Fe(III) precipitates, similar to the reference [7,27].

Fig. 4B shows that the independent P additions, though much smaller compared to Si (Table 1), results in a lower As(V) adsorption efficiency than with Si additions. These results can be explained by the pH dependent affinity of As(V), P and Si for the adsorption sites on Fe (III) precipitates [2,40,41] and the concentration differences between Si and P relative to As(V). The adsorption of As(V), Si and P onto the surface of Fe(III) precipitates is competitive. However, at pH 7.5 (this study), As(V) and P exhibit a similarly high affinity for adsorption sites on Fe(III) precipitates due to their negative charge and similar chemical properties. Silicate, on the other hand, is uncharged at pH 7.5 and the adsorption onto Fe(III) precipitates is much lower than As(V) and P. Thus, the greater reduction in As(V) adsorption due to lower P concentrations than Si is rationalized.

The As(V) removal efficiency was the lowest with the independent NOM additions. For example, the addition of 165 μM DOC resulted in As(V) removal efficiency of ≈ 20% and 35% after 1 min and 60 min, which decreased to 10% and 15% respectively with the independent addition of 500 μM DOC. The lower As(V) removal efficiency (Fig. 4A) compared to the reference was due to i) the lower adsorption of As(V) onto the surface of Fe(III) precipitates, as reflected in the lower As/Fe solids ratio for NOM additions (Fig. 4B), and ii) a higher mobility of Fe (III) due to the formation of Fe(III)–NOM complexes that were not removed by 0.45 μm filtration (Fig. 3). With NOM additions, the As/Fe solid ratio was higher than the As/Fe solid ratio with P additions. This indicates a stronger competition with As(V) for adsorption sites by P than NOM (Fig. 4B). Compared to the Si additions, the As/Fe solid ratio was slightly lower in case of NOM additions. This indicates a stronger competition with As(V) for adsorption sites by NOM than Si (Fig. 4B). Thus, in the given conditions, P competed with As(V) for adsorption sites on Fe(III) precipitates most strongly and reduced the As(V) adsorption followed by NOM, whereby Si showed had the least negative impact on As(V) adsorption.

From these results it can be concluded that the removal of As(V) in the presence of Si and P was affected mainly because of the reduced adsorption of As(V), whereas in the presence of NOM a reduced adsorption and a reduced Fe(III) removal both were responsible. Phosphate reduced As(V) adsorption the most, mainly because of its similar affinity for adsorption sites and higher concentration than As (V). But, the overall As(V) removal efficiency was reduced the most with the variations in NOM concentrations, mainly because NOM rendered a large portion of Fe(III) mobile in the solution.

3.2.2. Impact of combined Si, P and NOM additions

In the experiments where 165 μM DOC was fixed and P and Si concentrations were varied, the As(V) removal efficiency was lower than the reference experiment and the experiments with the corresponding independent Si, P and NOM additions (Fig. 4A). For example, with 165 μM DOC fixed, the addition of 1.3 μM P resulted in As(V) removal efficiency of 17 and 32% after 1 min and 60 min. This was lower than the As(V) removal efficiencies observed for the independent 1.3 μM P (25% and 44% after 1 min and 60 min) and 165 μM DOC (22% and 37% after 1 min and 60 min) additions. The lower As removal can be attributed to i) a greater competition for the adsorption of As(V) onto Fe(III) precipitates due to the presence of multiple inorganic and organic ions, as also confirmed by the lower As/Fe solid ratios, and ii) a NOM-induced higher mobility of Fe(III) (Fig. 3), as discussed previously.

At fixed P and NOM concentrations (1.3 μM P and 165 μM DOC), the addition of Si up to 280 μM resulted in only a slight reduction in As(V) removal efficiency compared to the absence of Si. Similarly, the removal efficiency of As(V) was reduced only slightly when P concentrations were increased up to 3.3 μM in the presence of 140 and 165 μM Si and DOC respectively. The subtle decrease in As(V) removal was attributed to a stronger competition for As(V) adsorption onto Fe (III) precipitates which resulted in a lower As/Fe solid ratio (Fig. 4B). Arsenate removal efficiency was majorly reduced with an increase in NOM concentration, with Si and P also present in water at fixed concentrations. For example, when 500 μM DOC was added along with 140 μM Si and 1.3 μM P, As(V) removal was reduced to zero. The absence of As(V) removal (Fig. 4A) was due to formation of Fe–NOM complexes that could not be filtered, as discussed previously.

Overall, it can be concluded that in complex solutions, containing Si, P, NOM and Ca, As(V) removal appears to be most sensitive to variations in NOM concentration, with NOM- Fe(III) complexation a key determinant.

3.2.3. Impact of removing anions and cations from RSF effluent

In the RSF effluent, the As(V) removal was lower than the reference experiment, i.e. As(V) removal was 46% in the RSF effluent compared to ≈ 90% for the reference solution after 60 min (Fig. 4A). The lower As (V) removal in RSF effluent compared to the reference was largely due to competition for As(V) adsorption from the anions such as Si, P and NOM. This was also confirmed by pre-treating the RSF effluent by AEX which showed that As(V) removal significantly increased with the removal of P and NOM (Table 1). The removal of Si with AEX treatment was not effective and therefore Si competed with As(V) for the adsorption sites, resulting in As/Fe solid ratio that matched the experiments where independent Si additions were investigated (Fig. 4B).

Arsenate removal was absent when the CEX-pre-treated RSF effluent was used as initial solution. The fact that no removal was observed in the absence of Ca and Mg is mainly due to the high mobility of Fe(III), which can be attributed to the highly negative surface of Fe(III) precipitates that hinders the growth of Fe(III) precipitates to become larger particles. The mechanistic understanding of how cations like Ca interact with Fe(III) precipitates in multi-anionic solutions has been presented in previous studies. It has been reported that when Ca is present during co-precipitation of Fe(III) and (oxy)anions such as Si, P, As(V) and NOM, it is incorporated in the structure of the growing Fe(III) precipitates due to chemical bonding with the surface-sorbed oxyanions [39]. Moreover, Ca interacts electrostatically with the surface of Fe(III) precipitates. Magnesium ions have also been shown to enhance aggregation of Fe(III) precipitates, but the effect is less pronounced than Ca [31,40].

4. Conclusions and implications for water treatment

This study shows that As(V) removal in Fe(III) based co-precipitation is sensitive to the composition of water matrix. In complex solutions containing multiple solutes and high levels of Ca, (variations in) Si and P concentrations reduce As(V) removal to some extent, mainly due to a decreased adsorption of As(V) onto Fe(III) precipitates. On the other hand, NOM concentrations reduce As(V) removal quite drastically, which we attribute largely to the formation of soluble and colloidal Fe(III)–NOM complexes.

The findings presented in this study have a great significance for predicting As removal at water treatment plants where water quality changes may take place, e.g. due to seasonal effects. Surface complexation modeling [10,17,21,22,36] is useful in gaining further insights in the As uptake by Fe(III) precipitates, but its application to real water treatment systems is limited. In water treatment plants, the effectiveness of As removal also depends on the separation of Fe(III) precipitates from water. Calcium effectively counteracts the negative effect of oxyanions and promotes the growth of Fe(III) precipitates, which can be easily separated from water by gravitation settling and rapid sand filtration. Thus, Ca-hardness of water should be carefully considered in designing As removal processes that rely on the co-precipitation of As and Fe. Obviously, effective separation of the colloidal particles can also be achieved by employing low-pressure membrane

filtration (MF/UF) instead of the conventional rapid sand filtration for effective separation of the colloidal particles. Nevertheless, also in this case, the charge and size distribution of Fe(III) precipitates will remain crucial in determining the membrane fouling mechanisms.

Declaration of Competing Interest

Authors declare that there is no conflict of interest.

Acknowledgement

This research is co-financed with PPS-funding from the Topconsortia for Knowledge & Innovation (TKI's) of the Ministry of Economic Affairs and Climate, The Netherlands. AA acknowledges support from Evides Waterbedrijf. The authors want to thank Wolter Siegers of KWR and Peter Vollaard of Evides for their support during the experiments.

Appendix A. Supplementary material

Supplementary data to this article can be found online at https://doi.org/10.1016/j.seppur.2019.116117.

References

[1] A. Ahmad, E. Cornelissen, S. van de Wetering, T. van Dijk, C. van Genuchten, J. Bundschuh, A. van der Wal, P. Bhattacharya, Arsenite removal in groundwater treatment plants by sequential Permanganate-Ferric treatment, J. Water Process Eng. 26 (2018) 221–229.
[2] A. Ahmad, B. van der Wal, P. Bhattacharya, C.M. van Genuchten, Characteristics of Fe and Mn bearing precipitates generated by Fe(II) and Mn(II) co-oxidation with O2, MnO4 and HOCl in the presence of groundwater ions, Water Res. (2019).
[3] C. Chen, J.J. Dynes, J. Wang, C. Karunakaran, D.L. Sparks, Soft X-ray spectromicroscopy study of mineral-organic matter associations in pasture soil clay fractions, Environ. Sci. Technol. 48 (12) (2014) 6678–6686.
[4] K.Y.-J. Choi, B.A. Dempsey, In-line coagulation with low-pressure membrane filtration, Water Res. 38 (19) (2004) 4271–4281.
[5] C.C. Davis, M. Edwards, Role of calcium in the coagulation of NOM with ferric chloride, Environ. Sci. Technol. 51 (20) (2017) 11652–11659.
[6] D.J. de Ridder, T.S.C.M. van de Wetering, T. van Dijk, D. van Halem, Influence of HPO_4^{2}, H_4SiO_4, Ca^{2+}, Mg^{2+} on Fe floc growth and As(III) removal in aerated, natural groundwater, J. Water Process Eng. 25 (2018) 149–156, https://doi.org/10.1016/j.jwpe.2018.07.004.
[7] S. Dixit, J.G. Hering, Comparison of arsenic(V) and arsenic(III) sorption onto iron oxide minerals: Implications for arsenic mobility, Environ. Sci. Technol. 37 (18) (2003) 4182–4189.
[8] E. Doelsch, J. Rose, A. Masion, J.Y. Bottero, D. Nahon, P.M. Bertsch, Speciation and crystal chemistry of Iron(III) chloride hydrolyzed in the presence of SiO_4 ligands. 1. An Fe K-edge EXAFS study, Langmuir 16 (10) (2000) 4726–4731.
[9] Haoran Dong, Xiaohong Guan, Dansi Wang, Jun Ma, Individual and combined influence of calcium and anions on simultaneous removal of chromate and arsenate by Fe(II) under suboxic conditions, Sep. Purif. Technol. 80 (2) (2011) 284–292, https://doi.org/10.1016/j.seppur.2011.05.007.
[10] D.A. Dzombak, F.M.M. Morel, Surface complexation modeling: hydrous ferric oxide, John Wiley & Sons, New York, New York, 1990.
[11] C.C. Fuller, J.A. Davis, G.A. Waychunas, Surface chemistry of ferrihydrite: Part 2. Kinetics of arsenate adsorption and coprecipitation, Geochim. Cosmochim. Acta 57 (10) (1993) 2271–2282.
[12] X. Guan, H. Dong, J. Ma, L. Jiang, Removal of arsenic from water: Effects of competing anions on As(III) removal in KMnO4–Fe(II) process, Water Res. 43 (15) (2009) 3891–3899.
[13] X. Guan, J. Ma, H. Dong, L. Jiang, Removal of arsenic from water: Effect of calcium ions on As(III) removal in the KMnO4–Fe(II) process, Water Res. 43 (20) (2009) 5119–5128.
[14] J.C.J. Gude, K. Joris, K. Huysman, L.C. Rietveld, D. van Halem, Effect of supernatant water level on As removal in biological rapid sand filters, Water Res. X 1 (2018) 100013.
[15] J.C.J. Gude, L.C. Rietveld, D. van Halem, Fate of low arsenic concentrations during full-scale aeration and rapid filtration, Water Res. 88 (2016) 566–574.
[16] J.G. Hering, P.-Y. Chen, J.A. Wilkie, M. Elimelech, S. Liang, Arsenic removal by ferric chloride, Am. Water Works Assoc. 88 (4) (1996) 155–167.
[17] T. Hiemstra, W.H. Van Riemsdijk, Surface structural ion adsorption modeling of competitive binding of oxyanions by metal (Hydr)oxides, J. Colloid Interface Sci. 210 (1) (1999) 182–193.
[18] A. Jain, K. Raven, R.H. Loeppert, Arsenite and arsenate adsorption on ferrihydrite: surface charge reduction and Net OH- release stoichiometry, Environ. Sci. Technol. 33 (8) (1999) 1179–1184.
[19] S. Jessen, F. Larsen, C.B. Koch, E. Arvin, Sorption and desorption of arsenic to ferrihydrite in a sand filter, Environ. Sci. Technol. 39 (20) (2005) 8045–8051.
[20] M. Kanematsu, T.M. Young, K. Fukushi, P.G. Green, J.L. Darby, Extended triple layer modeling of arsenate and phosphate adsorption on a goethite-based granular porous adsorbent, Environ. Sci. Technol. 44 (9) (2010) 3388–3394.
[21] M. Kanematsu, T.M. Young, K. Fukushi, P.G. Green, J.L. Darby, Arsenic(III, V) adsorption on a goethite-based adsorbent in the presence of major co-existing ions: Modeling competitive adsorption consistent with spectroscopic and molecular evidence, Geochim. Cosmochim. Acta 106 (2013) 404–428.
[22] E.J. Kim, B.-R. Hwang, K. Baek, Effects of natural organic matter on the coprecipitation of arsenic with iron, Environ. Geochem. Health 37 (6) (2015) 1029–1039.
[23] D. Lakshmanan, D. Clifford, G. Samanta, Arsenic removal by coagulation with aluminum, iron, titanium, and zirconium, Am. Water Works Assoc. 100 (2) (2008) 76–88.
[24] D. Laky, I. Licskó, Arsenic removal by ferric-chloride coagulation – effect of phosphate, bicarbonate and silicate, Water Sci. Technol. 64 (5) (2011) 1046–1055.
[25] Y. Masue, R.H. Loeppert, T.A. Kramer, Arsenate and arsenite adsorption and desorption behavior on coprecipitated aluminum: iron hydroxides, Environ. Sci. Technol. 41 (3) (2007) 837–842.
[26] T.D. Mayer, W.M. Jarrell, Formation and stability of iron(II) oxidation products under natural concentrations of dissolved silica, Water Res. 30 (5) (1996) 1208–1214.
[27] X. Meng, S. Bang, G.P. Korfiatis, Effects of silicate, sulfate, and carbonate on arsenic removal by ferric chloride, Water Res. 34 (4) (2000) 1255–1261.
[28] J. Qiao, Z. Jiang, B. Sun, Y. Sun, Q. Wang, X. Guan, Arsenate and arsenite removal by $FeCl_3$: Effects of pH, As/Fe ratio, initial As concentration and co-existing solutes, Sep. Purif. Technol. 92 (2012) 106–114.
[29] L.C. Roberts, S.J. Hug, T. Ruettimann, M.M. Billah, A.W. Khan, M.T. Rahman, Arsenic removal with Iron(II) and Iron(III) in waters with high silicate and phosphate concentrations, Environ. Sci. Technol. 38 (1) (2004) 307–315.
[30] J. Rose, A. Manceau, J.-Y. Bottero, A. Masion, F. Garcia, Nucleation and growth mechanisms of Fe oxyhydroxide in the presence of PO_4 ions. 1. Fe KEdge EXAFS study, Langmuir 13 (6) (1996) 1827–1834.
[31] A.-C. Senn, R. Kaegi, S.J. Hug, J.G. Hering, S. Mangold, A. Voegelin, Composition and structure of Fe(III)-precipitates formed by Fe(II) oxidation in water at near-neutral pH: Interdependent effects of phosphate, silicate and Ca, Geochim. Cosmochim. Acta 162 (2015) 220–246.
[32] P. Sharma, J. Ofner, A. Kappler, Formation of binary and ternary colloids and dissolved complexes of organic matter, Fe and As, Environ. Sci. Technol. 44 (12) (2010) 4479–4485.
[33] P.L. Smedley, D.G. Kinniburgh, A review of the source, behaviour and distribution of arsenic in natural waters, Appl. Geochem. 17 (5) (2002) 517–568.
[34] S. Sorlini, F. Gialdini, Conventional oxidation treatments for the removal of arsenic with chlorine dioxide, hypochlorite, potassium permanganate and monochloramine, Water Res. 44 (19) (2010) 5653–5659.
[35] G. Sposito, The chemistry of soils, Oxford University Press, New York, 2008.
[36] M. Stachowicz, T. Hiemstra, W.H. van Riemsdijk, Multi-competitive interaction of As(III) and As(V) oxyanions with Ca(2+), Mg(2+), PO(3-)(4), and CO(2-)(3) ions on goethite, J. Colloid Interface Sci. 320 (2) (2008) 400–414.
[37] C. Su, R.W. Puls, Arsenate and arsenite removal by zerovalent iron: effects of phosphate, silicate, carbonate, borate, sulfate, chromate, molybdate, and nitrate, relative to chloride, Environ. Sci. Technol. 35 (22) (2001) 4562–4568.
[38] C.M. van Genuchten, S.E.A. Addy, J. Peña, A.J. Gadgil, Removing arsenic from synthetic groundwater with iron electrocoagulation: An Fe and As K-Edge EXAFS study, Environ. Sci. Technol. 46 (2) (2012) 986–994.
[39] C.M. van Genuchten, A.J. Gadgil, J. Peña, Fe(III) nucleation in the presence of bivalent cations and oxyanions leads to subnanoscale 7 Å polymers, Environ. Sci. Technol. 48 (20) (2014) 11828–11836.
[40] C.M. Van Genuchten, J. Pena, S.E. Amrose, A.J. Gadgil, Structure of Fe(III) precipitates genberated by the electrolytric dissolution of Fe(0) in the presence of groundwater ions, Geochim. Cosmochim. Acta 127 (2014) 285–304.
[41] A. Voegelin, R. Kaegi, J. Frommer, D. Vantelon, S.J. Hug, Effect of phosphate, silicate, and Ca on Fe(III)-precipitates formed in aerated Fe(II)- and As(III)-containing water studied by X-ray absorption spectroscopy, Geochim. Cosmochim. Acta 74 (1) (2010) 164–186.
[42] G.A. Waychunas, B.A. Rea, C.C. Fuller, J.A. Davis, Surface chemistry of ferrihydrite: Part 1. EXAFS studies of the geometry of coprecipitated and adsorbed arsenate, Geochim. Cosmochim. Acta 57 (10) (1993) 2251–2269.
[43] L. Weng, W.H. Van Riemsdijk, T. Hiemstra, Humic nanoparticles at the oxide-water interface: Interactions with phosphate ion adsorption, Environ. Sci. Technol. 42 (23) (2008) 8747–8752.
[44] L. Weng, W.H. Van Riemsdijk, T. Hiemstra, Effects of fulvic and humic acids on arsenate adsorption to goethite: experiments and modeling, Environ. Sci. Technol. 43 (19) (2009) 7198–7204.
[45] J.A. Wilkie, J.G. Hering, Adsorption of arsenic onto hydrous ferric oxide: effects of adsorbate/adsorbent ratios and co-occurring solutes, Colloids Surf., A 107 (1996) 97–110.
[46] J. Youngran, M. Fan, J. Van Leeuwen, J.F. Belczyk, Effect of competing solutes on arsenic(V) adsorption using iron and aluminum oxides, J. Environ. Sci. 19 (8) (2007) 910–919.